

# Probe dependence on polar solvation dynamics from fs broadband fluorescence<sup>†</sup>

Tatu Kumpulainen, Arnulf Rosspeintner and Eric Vauthey<sup>\*</sup>

*Department of Physical Chemistry, University of Geneva,  
30 Quai Ernest Ansermet, Geneva, Switzerland*

Eric.Vauthey@unige.ch

## Electronic Supporting Information

Time-resolved fluorescence, best global fits, and residuals in EtOH.....	2
Band-shape parameters obtained from the global analysis in EtOH .....	3
Time-resolved fluorescence spectra, best global fits, and residuals of <b>C151</b> and <b>4AP</b> in DMSO and PhCN.....	4
Parameters of the solvent relaxation of <b>C151</b> and <b>4AP</b> .....	5
Estimated time-zero spectra and parameters of the Gaussians.....	6
Transition dipole moment representations in 2MB .....	7
Fluorescence anisotropy decays of <b>C151</b> and <b>4AP</b> .....	8
Decay parameters of the anisotropy decays .....	9
Example raw anisotropy decay dataset of <b>4AP</b> in PhCN .....	9
Time-resolved fluorescence of <b>C153</b> in EtOH .....	10
Comparison of the spectral relaxation functions and fluorescence anisotropy decays of <b>C151</b> and <b>4AP</b> in EtOH, DMSO, and PhCN.....	11
Estimation of the degree of specific solute-solvent interactions .....	12
References .....	13

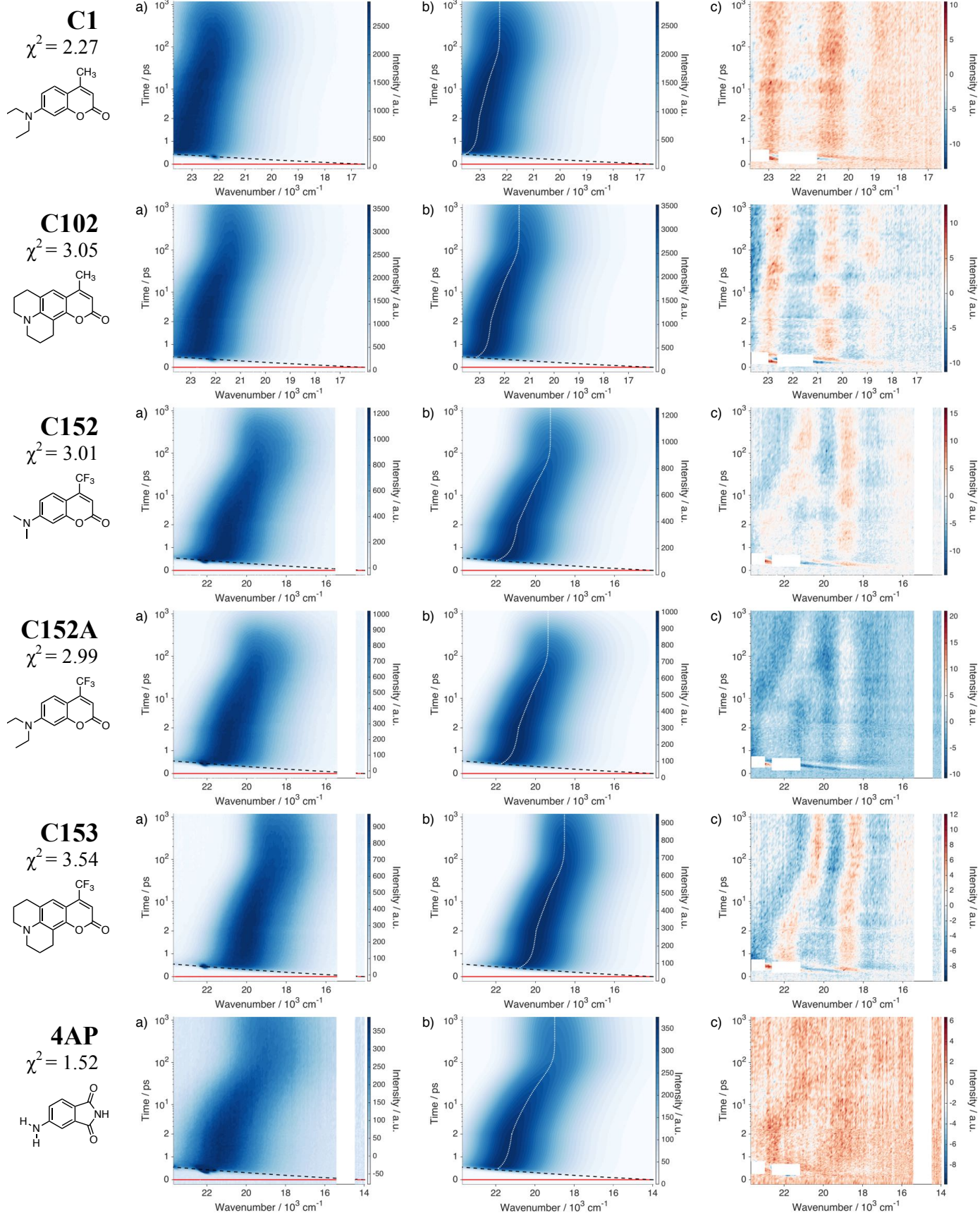


**Fig. S1** a) Time-resolved emission of (top to bottom) **C1**, **C102**, **C152**, **C152A**, **C153**, and **4AP** in EtOH ( $\lambda_{\text{exc.}} = 400$  nm); b) best global fits; and c) weighted residuals, on a lin-log time axis. The dashed black lines represent  $t = 0$  estimated from the chirp polynomial and the dashed white line the peak maxima. The blank white areas seen in the residuals are excluded from the fit and are due to the Raman scattering and third harmonic of the gate pulse.

**Table S1** Summary of the band-shape parameters of all compounds in EtOH obtained from the global analysis of the FLUPS data

compound	band integral, $A(t)$							$\tau_{fl}^a$ / ns
	$\alpha_1$ / %	$\tau_1$ / ps	$\alpha_2$ / %	$\tau_2$ / ps	$\alpha_3$ / %	$\tau_3$ / ns	$A_0$ / a.u.	
<b>C1</b>	3.1	2.9±0.7	6.0	63±5	90.9	3.3±0.1	9582	3.1±0.1
<b>C102</b>	3.1	4.1±0.7	14.8	55±2	82.1	4.9±0.1	11420	4.4±0.1
<b>C151</b>	4.4	1.6±0.2	9.5	50±2	86.1	5.2±0.1	5051	5.3±0.1
<b>C152</b>	7.0	1.3±0.1	15.9	27±1	77.1	1.8±0.1	5293	1.7±0.1
<b>C152A</b>	4.6	2.4±0.3	11.5	31±2	83.9	0.8±0.1	4127	0.8±0.1
<b>C153</b>	4.3	2.7±0.4	14.8	41±2	80.9	5.2±0.1	3868	4.7±0.1
<b>4AP</b>	6.8	5.7±0.8	17.8	44±3	75.5	9.9±0.5	1595	9.6±0.2

compound	width parameter, $\Delta x(t)$						in $\times 10^3$ cm <sup>-1</sup>	
	$\alpha_1$ / %	$\tau_1$ / ps	$\alpha_2$ / %	$\tau_2$ / ps	$\langle \tau \rangle^b$ / ps	$\Delta x_0$	$\Delta x_\infty$	$\Delta x_{tot}$
<b>C1</b>	100	2.3±0.3	—	—	2.3	2.99	2.88	-0.11
<b>C102</b>	71.2	1.7±0.2	28.8	141±42	42.0	2.95	2.83	-0.12
<b>C151</b>	46.9	1.6±0.2	53.1	45±3	24.4	3.80	3.35	-0.46
<b>C152</b>	14.9	1.4±0.6	85.1	48±4	41.5	3.81	3.55	-0.26
<b>C152A</b>	27.7	1.8±0.3	72.3	60±5	43.8	3.74	3.43	-0.31
<b>C153</b>	49.1	0.9±0.1	50.9	52±4	26.9	3.89	3.26	-0.62
<b>4AP</b>	—	—	—	—	—	3.89	3.89	0.00

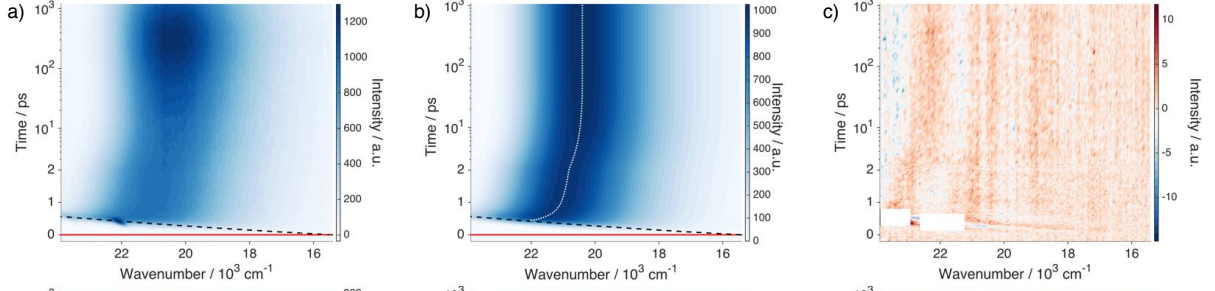
compound	asymmetry parameter, $b(t)$							
	$\alpha_1$ / %	$\tau_1$ / ps	$\alpha_2$ / %	$\tau_2$ / ps	$\langle \tau \rangle^b$ / ps	$b_0$	$b_\infty$	$\Delta b_{tot}$
<b>C1</b>	100	127±22	—	—	—	-0.30	-0.31	-0.02
<b>C102</b>	100	601±233	—	—	—	-0.30	-0.33	-0.02
<b>C151</b>	62.3	0.1±0.1	37.7	115±11	43	-0.20	-0.33	-0.13
<b>C152</b>	100	208±26	—	—	—	-0.25	-0.32	-0.06
<b>C152A</b>	100	142±16	—	—	—	-0.26	-0.33	-0.07
<b>C153</b>	52.7	0.7±0.2	47.3	182±28	86	-0.21	-0.33	-0.12
<b>4AP</b>	—	—	—	—	—	-0.23	-0.23	0.00

<sup>a</sup>Fluorescence lifetimes from ns-TCSPC measurements with ~200–300 ps IRF.

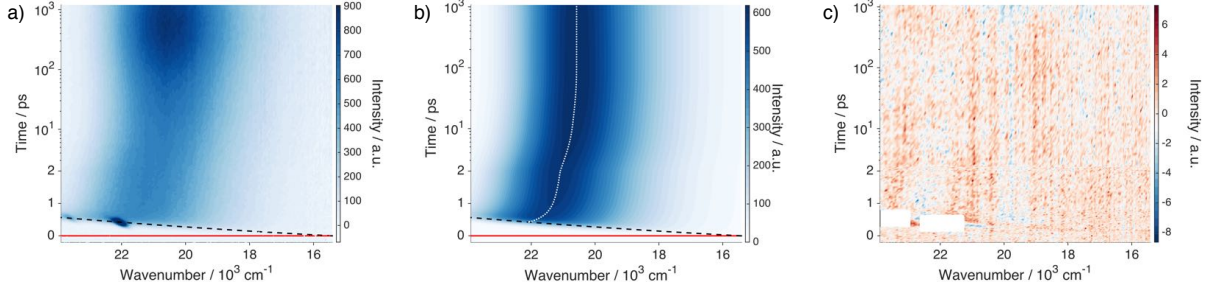
<sup>b</sup>Amplitude-weighted average lifetime,  $\langle \tau \rangle = \sum \alpha_i \tau_i$ .

## dimethyl sulfoxide (DMSO)

**C151**  
 $\chi^2 = 2.12$

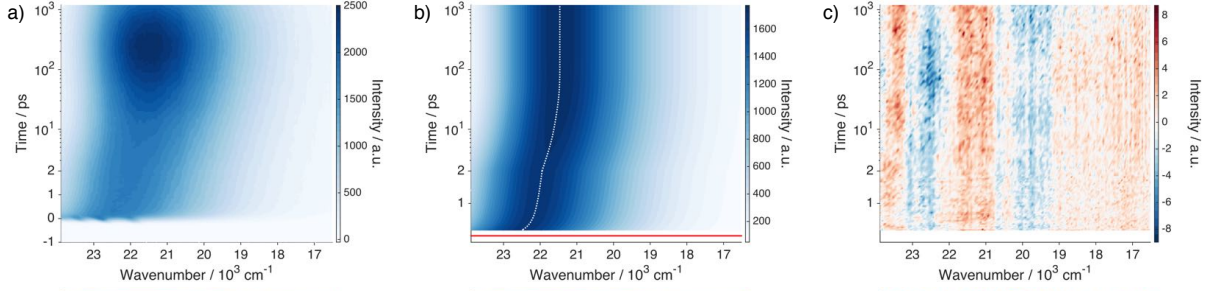


**4AP**  
 $\chi^2 = 1.67$



## benzonitrile (PhCN)

**C151**  
 $\chi^2 = 2.85$



**4AP**  
 $\chi^2 = 1.58$

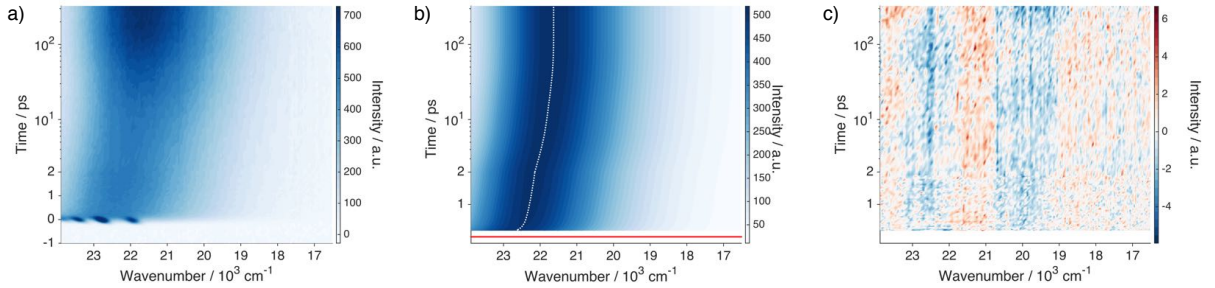


**Fig. S2** a) Time-resolved emission of **C151** and **4AP** in DMSO and PhCN ( $\lambda_{\text{exc.}} = 400$  nm); b) best global fits; and c) weighted residuals, on a lin-log time axis. The dashed white lines represent the fitted peak maxima. The blank white areas seen in the residuals are excluded from the fit and are due to the Raman scattering. The spectra were collected in a perpendicular polarization of the pump pulse to reduce the Raman scattering and further area-normalized prior to the global analysis. The data shown in a) represents the raw data i.e. before the normalization procedure. Due to strong Raman scattering signal in PhCN, the analyses were performed from  $t > 160$  fs on the chirp corrected data.

**Table S2** Parameters of the solvent relaxation of **C151** and **4AP** in all three solvents obtained from the global analysis of the FLUPS data. The values from ref. 1 for **C153** are included in the table for comparison. The total shift,  $\Delta\tilde{\nu}_{\text{tot}}$ , is given in units of  $\times 10^3 \text{ cm}^{-1}$ . Due to the strong Raman scattering, the analyses in PhCN were carried out from  $t \geq 160$  fs. Hence, both the amplitudes and lifetimes of the fastest components are subject to large errors and should be taken with caution. These components are, however, required to achieve adequate fits.

<b>compound</b>	<b>solvent</b>	$\alpha_1$	$\tau_1$ / ps	$\alpha_2$	$\tau_2$ / ps	$\alpha_3$	$\tau_3$ / ps	$\langle\tau\rangle^b$ / ps	$\Delta\tilde{\nu}_{\text{tot}}$
<b>C151</b>	EtOH	0.31	0.28	0.21	2.9	0.48	30.7	15.3	1.70
<b>C153<sup>a</sup></b>	<i>EtOH</i>	<i>0.23</i>	<i>0.27</i>	<i>0.25</i>	<i>4.9</i>	<i>0.52</i>	<i>29.9</i>	<i>16.7</i>	<i>1.95</i>
<b>4AP</b>	EtOH	0.17	0.42	0.21	4.4	0.61	40.2	25.7	2.96
<b>C151</b>	DMSO	0.53	0.22	0.35	1.9	0.11	9.0	1.8	1.74
<b>C153<sup>a</sup></b>	<i>DMSO</i>	<i>0.48</i>	<i>0.16</i>	<i>0.39</i>	<i>1.6</i>	<i>0.14</i>	<i>8.1</i>	<i>1.8</i>	<i>1.97</i>
<b>4AP</b>	DMSO	0.45	0.26	0.40	2.4	0.15	17.6	3.7	1.52
<b>C151</b>	PhCN	0.43	0.21	0.36	2.4	0.22	14.8	4.1	1.41
<b>C153<sup>a</sup></b>	<i>PhCN</i>	<i>0.38</i>	<i>0.22</i>	<i>0.49</i>	<i>4.63</i>	<i>0.13</i>	<i>20.6</i>	<i>5.0</i>	<i>1.17</i>
<b>4AP</b>	PhCN	0.52	0.11	0.31	2.3	0.16	19.3	3.9	1.84

<sup>a</sup>Values from Supplementary Table 1 of ref. 1.

<sup>b</sup>Amplitude-weighted average lifetime,  $\langle\tau\rangle = \sum \alpha_i \tau_i$ .



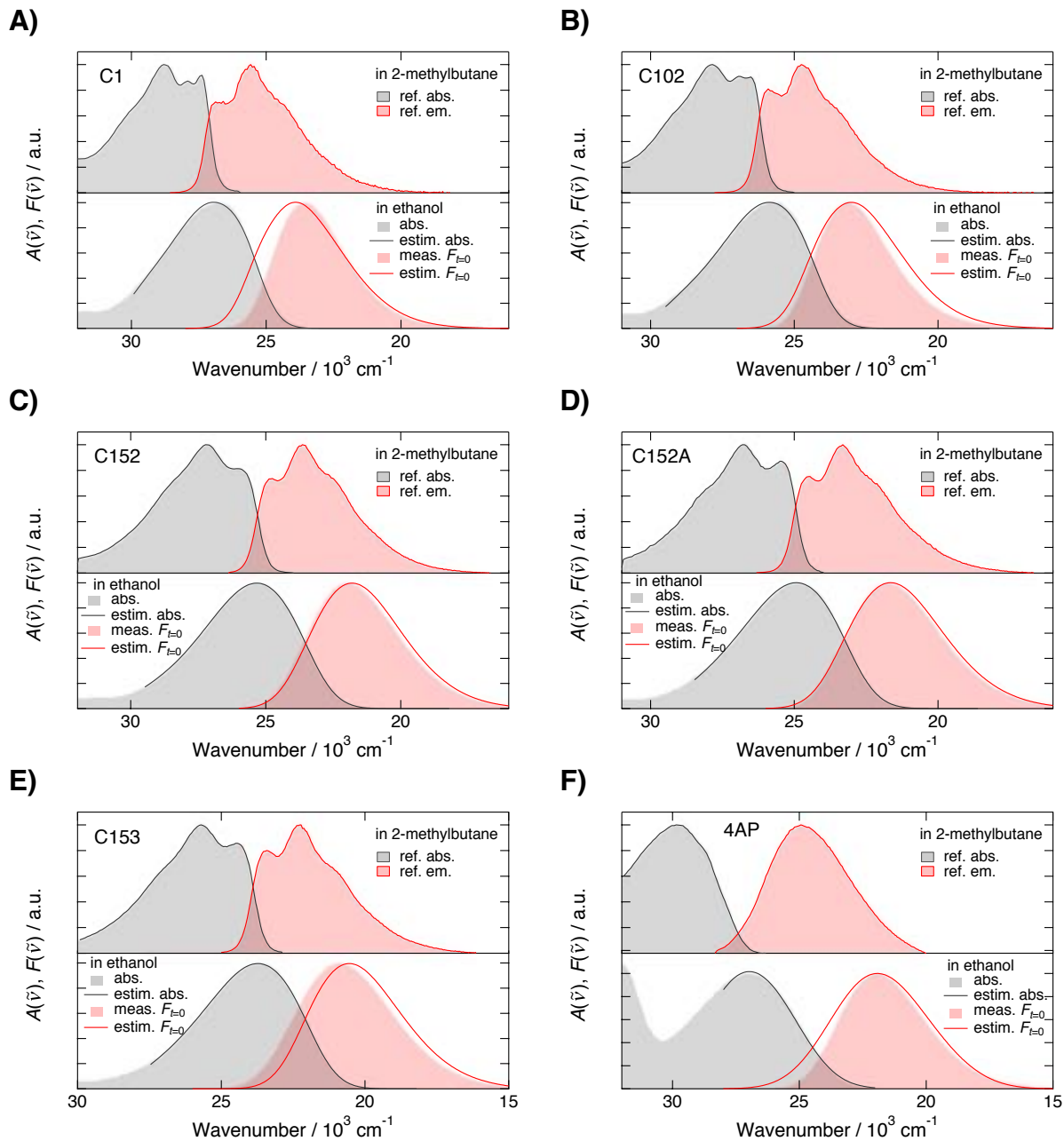


**Fig. S3** Top panels: Absorption (gray) and emission (red) spectra of the compounds in 2MB used to estimate the time-zero emission spectra in EtOH. Bottom panels: Measured (gray fill) and estimated (black line) absorption spectra together with the measured (red fill) and estimated (red line) time-zero emission spectra in EtOH. The measured time-zero emission spectra correspond to the spectra obtained from the global analyses of the FLUPS data at  $t = 0$ . The compounds are: A) C1; B) C102; C) C152; D) C152A; E) C153; and F) 4AP.

**Table S3** Parameters of the Gaussian used to estimate the time-zero emission spectra in EtOH. The intrinsic band-shape functions obtained from the spectra in nonpolar environment are convolved with the Gaussian. The shift,  $\delta_0$ , and the full-width half-maximum (FWHM),  $\Gamma_{inh}$ , of the Gaussian represent respectively the displacement and the broadening of the intrinsic band-shape function due to the polar environment. All parameters are given in  $10^3 \text{ cm}^{-1}$ .

compounds	C1	C102	C151	C152	C152A	C153	C153 <sup>a</sup>	4AP
shift, $\delta_0$	1.67	1.80	3.02	1.85	1.73	1.87	1.95	2.99
FWHM, $\Gamma_{inh}$	1.41	1.52	1.63	1.88	1.89	1.74	1.72	2.62

<sup>a</sup>Values from ref. 1.

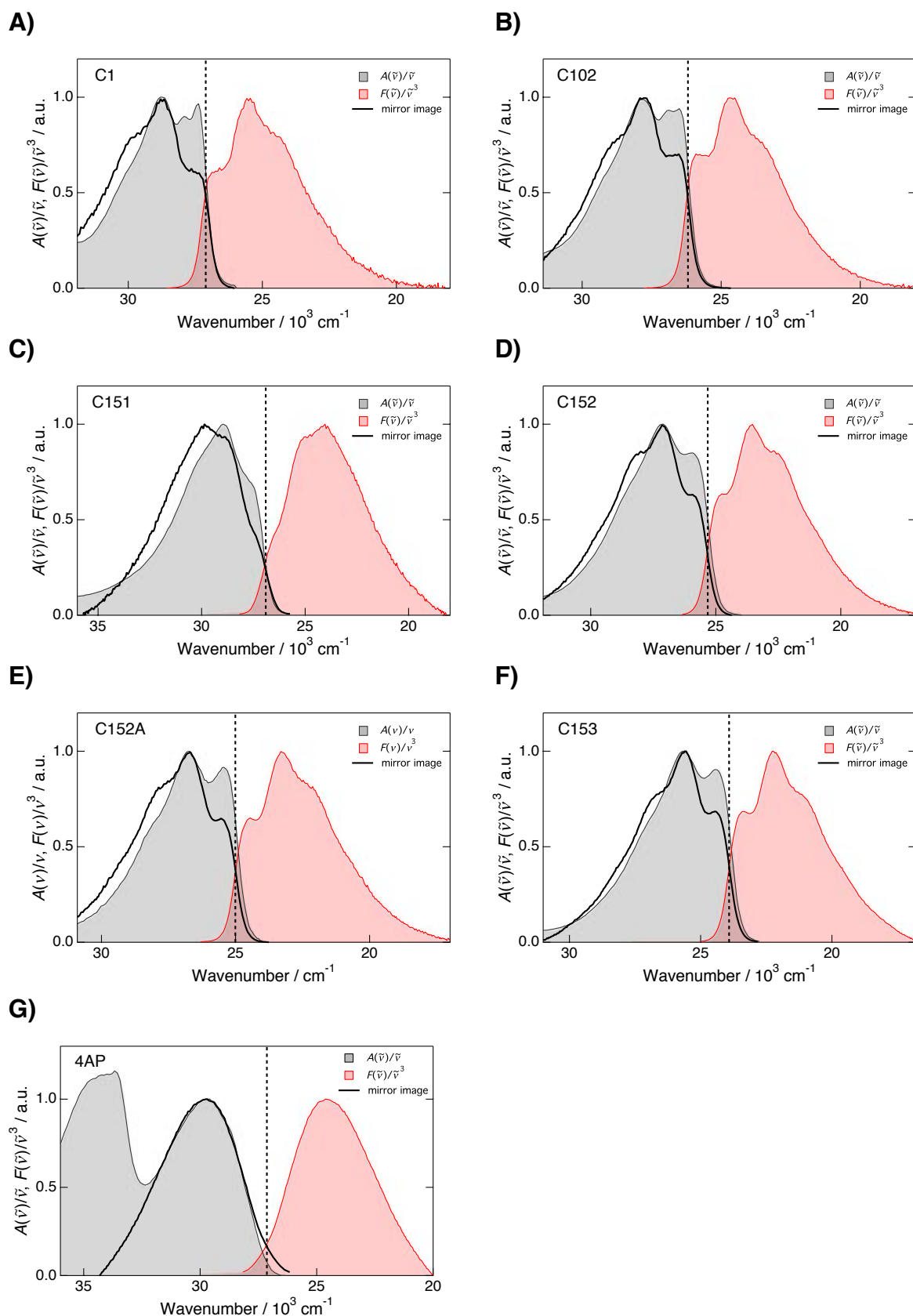


**Fig. S4** Transition dipole moment representations of the absorption (gray) and the emission (red) spectra of the compounds in 2MB used to estimate the spectra in EtOH. The black lines represent the mirror images of the emission transition dipole moment representations and allow direct comparison with the absorption representations. The compounds are: A) C1; B) C102; C) C151; D) C152; E) C152A; F) C153; and G) 4AP.

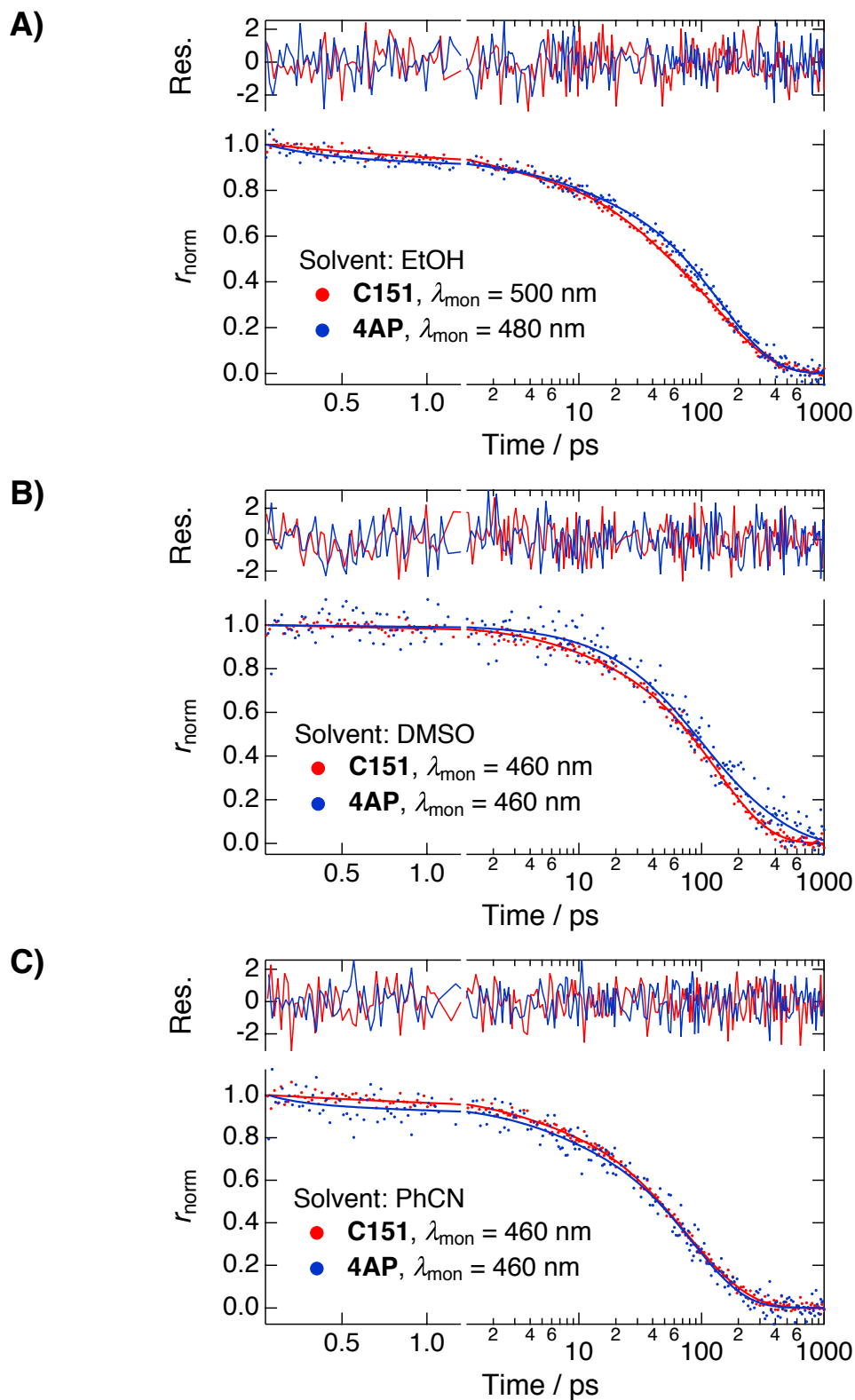


**Fig. S5** Intensity-normalized fluorescence anisotropy decays of **C151** (red) and **4AP** (blue) in A) EtOH, B) DMSO, and C) PhCN measured with a single wavelength fs fluorescence up-conversion setup. The excitation wavelength was 400 nm in EtOH and 390 nm in DMSO and PhCN. The monitoring wavelengths are indicated in the figures. The points represent the measured anisotropy decays as obtained from the decays measured at the parallel and perpendicular polarization of the pump (see eq. (9) in the main text). The lines represent the best fits of two- or three-exponential functions. The top panels show the weighted residuals.



**Table S4** Fluorescence anisotropy decay parameters of **C151** and **4AP** in EtOH, DMSO, and PhCN obtained from multi-exponential analyses. All datasets were analyzed from  $t \geq 50$  fs.

	solvent	$\alpha_1$	$\tau_1$ / ps	$\alpha_2$	$\tau_2$ / ps	$\alpha_3$	$\tau_3$ / ps	$\langle \tau \rangle^a$ / ps	$r_0$	$\chi^2$
<b>C151</b>	EtOH	0.10	$1.5 \pm 0.6$	0.22	$25 \pm 6$	0.68	$150 \pm 10$	109	0.39	1.06
<b>4AP</b>	EtOH	0.08	$0.4 \pm 0.3$	0.10	$8 \pm 4$	0.82	$144 \pm 7$	119	0.39	1.01
<b>C151</b>	DMSO	–	–	0.09	$8 \pm 4$	0.91	$134 \pm 5$	122	0.38	1.05
<b>4AP</b>	DMSO	–	–	0.53	$70 \pm 30$	0.47	$290 \pm 120$	173	0.35	1.23
<b>C151</b>	PhCN	0.09	$3.0 \pm 1.6$	0.26	$40 \pm 30$	0.65	$100 \pm 20$	77	0.38	1.03
<b>4AP</b>	PhCN	0.06	$0.2 \pm 0.5$	0.11	$5 \pm 3$	0.83	$84 \pm 4$	70	0.39	0.92

<sup>a</sup>Amplitude-weighted average lifetime,  $\langle \tau \rangle = \sum \alpha_i \tau_i$ .

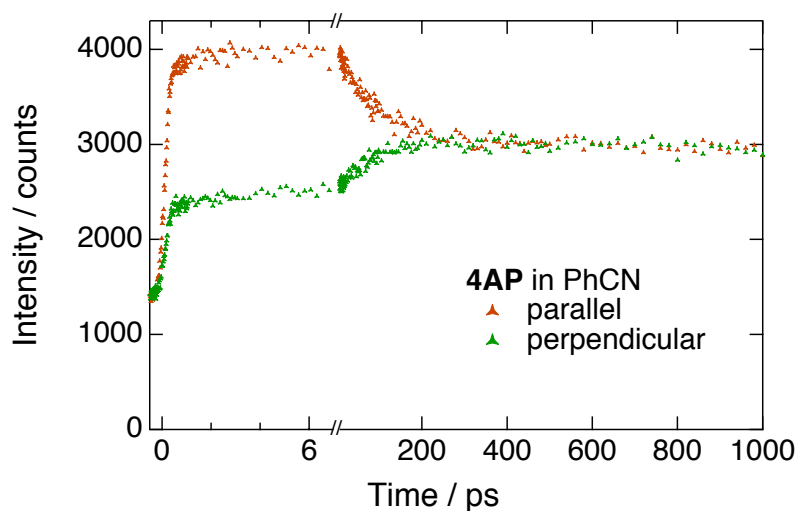


**Fig. S6** Example raw fluorescence anisotropy data measured with **4AP** in PhCN using a single wavelength fs fluorescence up-conversion setup at parallel and perpendicular polarizations of the pump pulse. The excitation and the monitoring wavelengths were 390 nm and 460 nm, respectively. The large number of counts before  $t = 0$  are due to the relatively long lifetime of **4AP** in aprotic organic solvents and the high repetition rate of the laser system ( $\sim 80$  MHz).

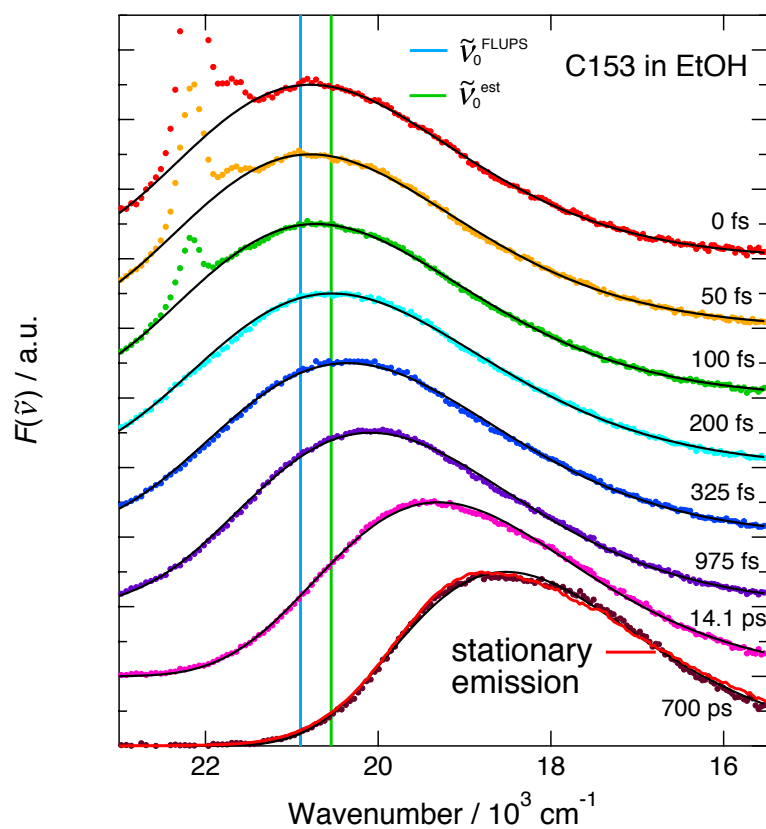


**Fig. S7** Time evolution of the fluorescence of **C153** in EtOH. The markers indicate the data points and the black solid lines are the best-fits of log-normal functions. The observed and the estimated time-zero peak frequencies are indicated by vertical blue and green lines, respectively. The stationary emission spectrum (red solid line) is overlaid with the time-resolved spectrum measured at 700 ps.

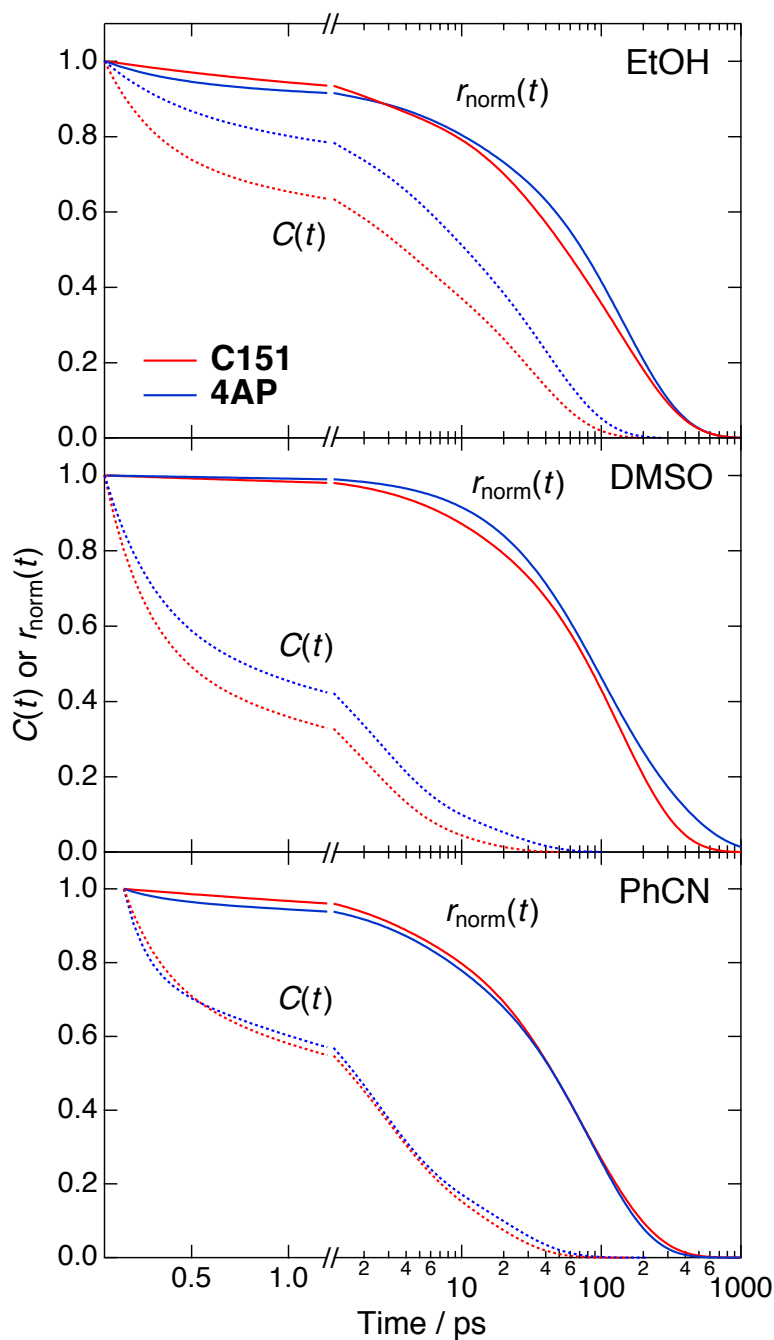


**Fig. S8** Comparison of the solvent relaxation functions,  $C(t)$ , and the fluorescence anisotropy decays,  $r_{\text{norm}}(t)$ , of **4AP** and **C151** in EtOH, DMSO, and PhCN. The decays are normalized to one at  $t = 50$  fs in EtOH and DMSO. In PhCN, the decays are normalized at  $t = 160$  fs due to the limited fitting range of the FLUPS data. All decays presented above are obtained from the fits of multi-exponential functions. The decay parameters are given in Table S2 for  $C(t)$  and in Table S4 for  $r(t)$ .

## Estimation of the degree of specific interactions using simple hydrodynamic theory

The average rotational times were determined both experimentally and theoretically. The amplitude-weighted average lifetimes were used as the experimental values whereas the theoretical values were calculated using the Stokes-Einstein-Debye (SED) model<sup>2,3</sup>

$$\tau_{\text{rot}} = \frac{VfC\eta}{k_{\text{B}}T} \quad (1)$$

where  $V$  is the volume of the solute,  $f$  is a factor accounting for the nonspherical shape of the solute,  $\eta$  is the viscosity of the solvent,  $k_{\text{B}}$  is the Boltzmann's constant,  $T$  is the temperature and  $C$  is the coupling parameter. Usually, the coupling parameter,  $C$ , is determined for a series of solvents and represents the deviation from the SED prediction.

In our case, we will make a simple comparison by assuming that  $f$  and  $C$  are equal to one. The calculated rotational times are compared with the average lifetimes of the measured fluorescence anisotropy decays and the difference, roughly speaking, represent the deviation from the SED prediction. The molecular volumes were obtained from DFT calculations on optimized ground-state geometries using the *volume* keyword. All calculations were performed on the B3LYP level of theory with the 6-31+G(d,p) basis set. All relevant parameters are summarized in Table S5.

As seen in Table S5, the agreement between the observed and predicted rotational times of **C151** in PhCN and DMSO is good whereas the predicted time is significantly smaller in ethanol. This indicates that only the hydrogen bonds donated by the solvent will significantly influence the rotational dynamics. This is expected due to the charge-transfer character of the coumarins. The hydrogen bonds donated by the  $-\text{NH}_2$  group are cleaved in the excited state whereas those accepted by the carbonyl oxygen are strengthened. **4AP**, on the other hand, shows deviations from the predicted values in all three solvents. The deviation is largest in DMSO indicating that the strong hydrogen bonds to the amine hydrogens will significantly decelerate the rotational dynamics. Thus, it can be argued that these hydrogen bonds, persisting in the excited state, will also decelerate the solvent relaxation in agreement with the observations. In EtOH, both compounds are decelerated by the specific interactions but the magnitude is larger for **4AP**. This is again translated into slower solvent relaxation. In PhCN, both compounds show a relatively good agreement between the observed and predicted rotational times indicating no or only weak specific solute-solvent interactions and the observed solvation times are nearly equal.

The above explanations based on the rotational dynamics are merely qualitative but nevertheless support the conclusion that the differences in the solvent relaxation can be attributed to specific solute-solvent interactions. Much larger dataset would be, however, required for a quantitative investigation.

**Table S5** Parameters used to estimate the rotational times using the SED model.  $\langle\tau_{\text{rot}}\rangle$  is the average rotational time from the fluorescence anisotropy decays,  $\tau_{\text{SED}}$  the value calculated from the SED model and  $R_{\text{rot}}$  the ratio of the two. The average solvation times,  $\langle\tau_{\text{solv}}\rangle$ , are included for comparison.

	solvent	$\eta$ / cP	$V$ / Å <sup>3</sup>	$\langle\tau_{\text{rot}}\rangle$ / ps	$\tau_{\text{SED}}$ / ps	$R$	$\langle\tau_{\text{solv}}\rangle$ / ps
<b>C151</b>	EtOH	1.08	260	109	69	1.6	15.3
<b>4AP</b>	EtOH	1.08	182	119	48	2.5	25.7
<b>C151</b>	DMSO	1.99	260	122	127	1.0	1.8
<b>4AP</b>	DMSO	1.99	182	173	89	1.9	3.7
<b>C151</b>	PhCN	1.24	260	77	79	1.0	4.1
<b>4AP</b>	PhCN	1.24	182	70	55	1.3	3.9

## References:

- (1) Horng, M. L.; Gardecki, J. A.; Papazyan, A.; Maroncelli, M. *J. Phys. Chem.* **1995**, *99* (48), 17311–17337.
- (2) Evans, G. T.; Kivelson, D. *J. Chem. Phys.* **1986**, *84* (1), 385–390.
- (3) Horng, M. L.; Gardecki, J. A.; Maroncelli, M. *J Phys Chem A* **1997**, *101* (6), 1030–1047.